

Photoionization spectra of CH₃I and C₂H₅I perturbed by CF₄ and *c*-C₄F₈: Electron scattering in halocarbon gases

C. M. Evans^{1,2,3}, E. Morikawa² and G. L. Findley^{3,*}

¹*Department of Chemistry, Louisiana State University, Baton Rouge, LA 70809*

²*Center for Advanced Microstructures and Devices (CAMD), Louisiana State University, Baton Rouge, LA 70806*

³*Department of Chemistry, University of Louisiana at Monroe, Monroe, LA 71209*

(submitted May 10, 2000)

Photoionization spectra of CH₃I and C₂H₅I doped into perturber halocarbon gases CF₄ (up to a perturber number density of $6.1 \times 10^{20} \text{ cm}^{-3}$) and *c*-C₄F₈ (up to a perturber number density of $2.42 \times 10^{19} \text{ cm}^{-3}$) disclosed a red shift of the dopant autoionizing features that depends linearly on the perturber number density. In the case of CF₄, which is transparent in the spectral region of interest, this red shift was verified from the dopant photoabsorption features as well. From the perturber-induced energy shifts of the dopant Rydberg states and ionization energies, the zero-kinetic-energy electron scattering lengths for CF₄ and *c*-C₄F₈ were found to be $-0.180 \pm 0.003 \text{ nm}$ and $-0.618 \pm 0.012 \text{ nm}$, respectively. To our best knowledge, these are the first measurements of zero-kinetic-energy electron scattering lengths for both CF₄ and *c*-C₄F₈. From these zero-kinetic-energy electron scattering lengths, we find that the zero-kinetic-energy electron scattering cross-sections are $\sigma = 4.1 \pm 0.2 \times 10^{-15} \text{ cm}^2$ and $4.8 \pm 0.2 \times 10^{-14} \text{ cm}^2$ for CF₄ and *c*-C₄F₈, respectively.

PACS number(s): 33.20.Ni, 34.80.-i

I. Introduction

The interaction of halocarbon gases like CF₄ and *c*-C₄F₈ with low energy [1-4] and high energy electrons [3,5,6] has received increasing attention, primarily due to the importance of these gases to the semiconductor industry [3], and to the involvement of these gases in stratospheric photochemistry [7]. In fact, many of the perfluorinated halocarbons are used as sources for reactive species in plasma etching [8,9], and halocarbons have the potential to be used as insulators in high voltage switches [4].

In order to model accurately the behavior of halocarbon gases in both plasma etching and stratospheric photochemistry, the interaction between halocarbons and low energy electrons must be better understood. However, the measurement of low energy electron scattering cross-sections and low energy electron attachment rates for halocarbons can be extremely difficult because of the large electronegativities of these molecules. For example, a typical method for studying

electron/gas interactions, the electron swarm method, depends on the electron number density remaining constant throughout the experiment [10]. When a molecule has a large electronegativity, however, the electron number density will vary during the experiment as a result of electron attachment in addition to electron induced ionization, thus complicating the interpretation of data [10]. For such molecular species, the measurement of zero-kinetic-energy electron scattering cross-sections is particularly problematic [3,4,10]. As a result, many numerical calculations have predicted the zero-kinetic-energy cross-section of CF₄ [1,3,5,11,12] with an emphasis on extension to other halogenated gases. However, the accuracy of these calculated values is currently unknown since, to the best of our knowledge, no zero-kinetic-energy electron scattering cross-section measurements have been obtained for CF₄.

An alternative method for determining the zero-kinetic-energy electron scattering cross-section of a gas involves perturber-induced energy shifts of high-*n* Rydberg states [13-19] of

a dopant molecule. In this method, a dopant molecule having a Rydberg series observable in photoabsorption and/or photoionization spectroscopy is mixed with a perturber gas of interest. As the perturber concentration is increased, the dopant high- n Rydberg state energies shift as a result of dopant/perturber interactions. These energy shifts can then be modeled using a theory by Fermi [14], as modified by Alekseev and Sobel'man [15]. According to these authors [14,15], the total energy shift Δ can be written as a sum of contributions

$$\Delta = \Delta_{\text{sc}} + \Delta_{\text{p}}, \quad (1)$$

where Δ_{sc} is the scattering shift resulting from the interactions of the optical electron with the perturber medium, and Δ_{p} is the polarization shift resulting from the interaction of the dopant core with the perturber medium. Δ_{p} can be computed from [13,15]

$$\Delta_{\text{p}} = -10.78 \left(\frac{1}{2} \alpha e^2 \right)^{2/3} (\hbar v)^{1/3} \rho, \quad (2)$$

where ρ is the perturber number density, α is the polarizability of the perturber molecule, e is the charge on the electron, \hbar is the reduced Planck constant, and v is the relative thermal velocity of the dopant and perturber molecules. Δ_{sc} results from a measurement of Δ , after calculating Δ_{p} . Finally, the electron scattering length A of the perturber, which gauges the electron-perturber interactions, can be determined from [14]

$$\Delta_{\text{sc}} = \left(\frac{2 \pi \hbar^2}{m} \right) A \rho, \quad (3)$$

where m is the mass of the electron. The zero-kinetic-energy electron scattering cross-section is then related to the zero-kinetic-energy electron scattering length by [14]

$$\sigma = 4 \pi A^2. \quad (4)$$

The perturber-induced energy shifts of high- n Rydberg states have been used to obtain the zero-kinetic-energy electron scattering lengths of numerous gases [16,17], including the

electronegative gases CO_2 [18] and SF_6 [17,19].

In the present Paper, we present photoionization spectra of the dopant molecules CH_3I and $\text{C}_2\text{H}_5\text{I}$ perturbed by CF_4 , as well as photoionization spectra of CH_3I perturbed by $c\text{-C}_4\text{F}_8$. Since $c\text{-C}_4\text{F}_8$ weakly absorbs in the same energy region as the first and second ionization energies of both CH_3I and $\text{C}_2\text{H}_5\text{I}$, measurements of photoabsorption spectra are not possible with this perturber except for very low pressures of $c\text{-C}_4\text{F}_8$. CF_4 , however, is transparent in this spectral region and, therefore, photoabsorption spectra of CH_3I and $\text{C}_2\text{H}_5\text{I}$ doped into CF_4 are also presented.

From the measured perturber-induced energy shifts of dopant high- n Rydberg states, and from the corresponding dopant ionization energy shifts obtained by fitting energy levels to the Rydberg equation, we extract the zero-kinetic-energy electron scattering lengths of CF_4 and $c\text{-C}_4\text{F}_8$, which are then used to compute the zero-kinetic-energy electron scattering cross-sections. To the best of our knowledge, this is the first measurement of the zero-kinetic-energy electron scattering length for either of these gases. For the case of CF_4 , we compare our measured zero-kinetic-energy electron scattering cross-section with the theoretical values computed from various methods [3,12].

2. Experiment

Photoionization and photoabsorption spectra were measured with monochromatic synchrotron radiation [20] (with a resolution of 0.09 nm, or ~ 8 meV in the spectral region of interest), which entered a copper experimental cell [17,21] equipped with entrance and exit MgF_2 windows. This cell, which is capable of withstanding pressures of up to 100 bar, possesses two parallel plate electrodes (stainless steel, 3 mm spacing) aligned perpendicular to the windows, thus allowing for the simultaneous measurement of photoionization and transmission spectra. The light path within the

cell is 1.0 cm, and all transmission spectra were below saturation (which was verified by measuring selected spectra at different dopant pressures). The applied voltage was 100 V, and all photoionization spectra were current saturated (which was verified by measuring selected spectra at different applied voltages). Photocurrents within the cell were of the order of 10^{-10} A.

The intensity of the synchrotron radiation exiting the monochromator was monitored by measuring the current across a metallic mesh intercepting the beam prior to the experimental cell. All photoionization spectra are normalized to this current. All transmission spectra (reported here as absorption = 1 - transmission) are normalized both to the incident light intensity and to the empty cell transmission. Spectral energy calibrations were performed by comparison of the low pressure spectra of the pure dopants with previously published spectra (see [22]).

CH_3I (Aldrich Chemical, 99.5%), $\text{C}_2\text{H}_5\text{I}$ (Sigma, 99%), CF_4 (Matheson Gas Products, 99.999%) and $c\text{-C}_4\text{F}_8$ (Matheson Gas Products, 99.98%) were used without further purification. Both the gas handling system and the procedures employed to ensure homogeneous mixing of the dopant and perturber have been described previously [17,22,23]. The dopant pressures measured in the gas handling system were reproducible to within ± 0.01 mbar, and the perturber pressures were reproducible to within ± 0.1 bar for the high number density range [22].

3. Results and Discussions

Photoionization measurements of CH_3I and CH_3I doped into varying number densities of CF_4 are presented in Fig. 1 in the autoionizing region [16] ($I_1 < h\nu < I_2$) of CH_3I . In Fig. 2, photoabsorption measurements of $\text{C}_2\text{H}_5\text{I}$ and $\text{C}_2\text{H}_5\text{I}$ doped into varying number densities of CF_4 are shown. (The measured photoionization

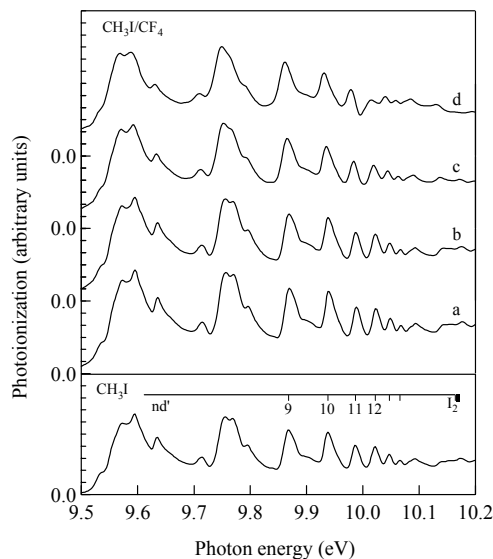


FIG 1. Photoionization spectra ($T = 25^\circ\text{C}$) of pure CH_3I (0.1 mbar), and CH_3I (0.1 mbar) doped into varying number densities (10^{20} cm^{-3}) of CF_4 : (a) 0.073; (b) 0.23; (c) 0.74 and (d) 1.30. All spectra are intensity normalized to the same spectral feature above the CH_3I ${}^2\text{E}_{3/2}$ ionization limit.

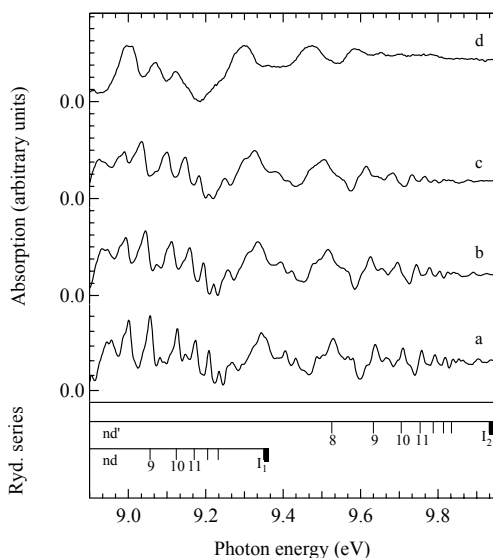


FIG 2. Photoabsorption spectra of $\text{C}_2\text{H}_5\text{I}/\text{CF}_4$ at 25°C . Photoabsorption spectra of (a) 0.5 mbar $\text{C}_2\text{H}_5\text{I}$, and $\text{C}_2\text{H}_5\text{I}$ doped into varying number densities of CF_4 (10^{20} cm^{-3}): b, 1.22; c, 2.43; d, 6.08. The concentration of $\text{C}_2\text{H}_5\text{I}$ was kept below 10 ppm in CF_4 . All absorption spectra are corrected for the empty cell transmission. The assignment given at the bottom corresponds to the pure $\text{C}_2\text{H}_5\text{I}$ spectrum.

spectra of C_2H_5I doped into CF_4 , and the photoabsorption spectra of CH_3I doped into CF_4 are not shown for the sake of brevity.) The values of I_2 ($\equiv I(^2E_{1/2})$ [16]) obtained from fitting the assigned CH_3I photoionization spectra to the Rydberg equation (according to the procedures described in [16]) are given in Table 1, along with the values for I_2 ($\equiv I(\tilde{X}_2^2E_{1/2})$ [24,25]) extracted from the C_2H_5I photoionization spectra. Although the measured spectra are not shown here, we have also included in Table 1 the values of I_1 ($\equiv I(\tilde{X}_1^2E_{1/2})$ [24,25]) and I_2 extracted from the C_2H_5I photoabsorption measurements, and I_1 ($\equiv I(^2E_{3/2})$ [16]) and I_2 extracted from the CH_3I photoabsorption measurements. In Fig. 3 we present the photoionization spectra of CH_3I and CH_3I doped into varying number densities of $c-C_4F_8$. Photoabsorption measurements, however, were not possible due to the absorption of $c-C_4F_8$ in this spectral region. In Table 2, the values of I_2 extracted from fitting the assigned CH_3I photoionization spectra to the Rydberg equation are given. (The values of the energy positions

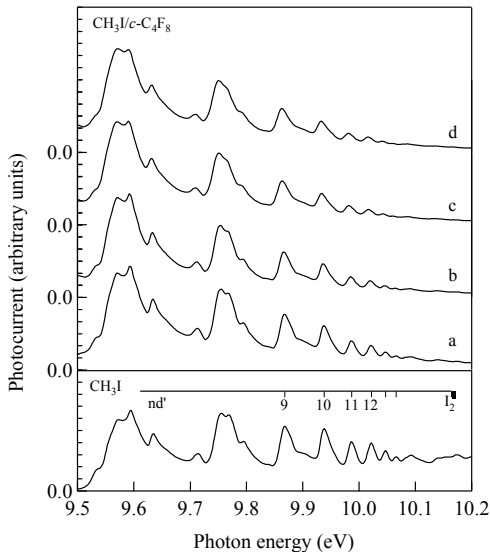


FIG 3. Photoionization spectra ($T = 25^\circ C$) of pure CH_3I (0.1 mbar) and CH_3I (0.1 mbar) doped into varying number densities (10^{19} cm^{-3}) of $c-C_4F_8$: (a) 0.12; (b) 0.73; (c) 1.81 and (d) 2.42. All spectra are intensity normalized to the same spectral feature above the CH_3I $^2E_{3/2}$ ionization limit.

Table 1. Selected first ionization energies (obtained from photoabsorption (PA) measurements) and second ionization energies (obtained from photoabsorption and photoionization (PI) measurements) of CH_3I and C_2H_5I doped into various number densities ρ (10^{20} cm^{-3}) of CF_4 . All ionization energies are in eV.

CH₃I			
ρ	I_1 (PA)	I_2 (PA)	I_2 (PI)
0.039	9.537	10.164	10.164
0.073	9.536	10.163	10.163
0.23	9.535	10.162	10.162
0.74	9.532	10.158	10.158
1.30	9.527	10.153	10.153
C₂H₅I			
ρ	I_1 (PA)	I_2 (PA)	I_2 (PI)
0.24	9.346	9.930	9.930
1.21	9.339	9.921	9.921
2.39	9.329	9.913	9.913
4.60	9.309	9.894	9.894
6.10	9.296	9.880	

of the nd and nd' Rydberg states used to obtain the ionization energies presented in Tables 1 and 2 are collected in [22].)

A plot of the shift in ionization energy ΔI as a function of the number density ρ of CF_4 is shown in Fig. 4. Fig. 4 demonstrates that the red shift of the ionization energy depends linearly upon the perturber number density and, therefore, can be analyzed within the Fermi model (cf. eqs. (1) - (3)). (Analogous plots for the various Rydberg state energies yield correlations in every case which are parallel (to within experimental error) to the correlation line of Fig. 4.) The slope of the linear fit (obtained by regression analysis) of Fig. 4 is $\Delta/\rho = -8.648 \pm 0.172 \times 10^{-23} \text{ eV cm}^3$. Using the value [26] $\alpha = 3.838 \times 10^{-24} \text{ cm}^3$ for CF_4 in eq. (2) gives a polarization shift of $\Delta_p/\rho = -3.38 \times 10^{-26} \text{ eV cm}^3$. Substituting Δ_p/ρ and Δ/ρ into eq. (1) leads to $\Delta_{sc}/\rho = -8.646 \pm 0.172 \times 10^{-23} \text{ eV cm}^3$ which, when substituted into eq. (3), gives a zero-

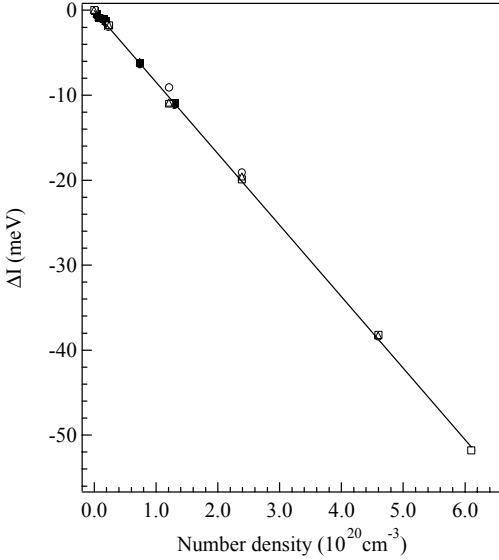


FIG 4. Shifts of the ionization energies of CH_3I and $\text{C}_2\text{H}_5\text{I}$, obtained from fitting the assigned spectra (e.g., Figs. 1 and 2) to the Rydberg equation, as a function of CF_4 number density. \bullet , I_1 CH_3I photoabsorption; \blacksquare , I_2 CH_3I photoabsorption; \blacktriangle , I_2 CH_3I photoionization; \circ , I_1 $\text{C}_2\text{H}_5\text{I}$ photoabsorption; \square , I_2 $\text{C}_2\text{H}_5\text{I}$ photoabsorption; \triangle , I_2 $\text{C}_2\text{H}_5\text{I}$ photoionization. (The error in the energy for each point is ± 3 meV.)

kinetic-energy scattering length of $A = -0.180 \pm 0.003$ nm. Therefore, the zero-kinetic-energy electron scattering cross-section [cf. eq. (4)] is $\sigma = 4.1 \pm 0.2 \times 10^{-15} \text{ cm}^2$. Current estimates of low energy electron scattering cross-sections for CF_4 range from a low of $1.269 \times 10^{-15} \text{ cm}^2$, obtained by averaging all of the currently known low energy electron scattering cross-section measurements [3], to a high of $8 \times 10^{-15} \text{ cm}^2$ [12] computed using the continuum MS- $X\alpha$ method described by Davenport [27]. The value we obtain for the zero-kinetic-energy cross-section, therefore, falls within these two limits.

Similar to the above analysis, Fig. 5 presents the change in the ionization energy of CH_3I as a function of $c\text{-C}_4\text{F}_8$ number density ρ . As was the case for CF_4 , a red shift which is linearly dependent upon the $c\text{-C}_4\text{F}_8$ number density is observed. The slope of the straight line (obtained from regression analysis) is $\Delta/\rho = -29.57 \pm 0.51 \times 10^{-23} \text{ eV cm}^3$. Using the value [87] $\alpha = 7.37 \times 10^{-24} \text{ cm}^3$ for $c\text{-C}_4\text{F}_8$, and

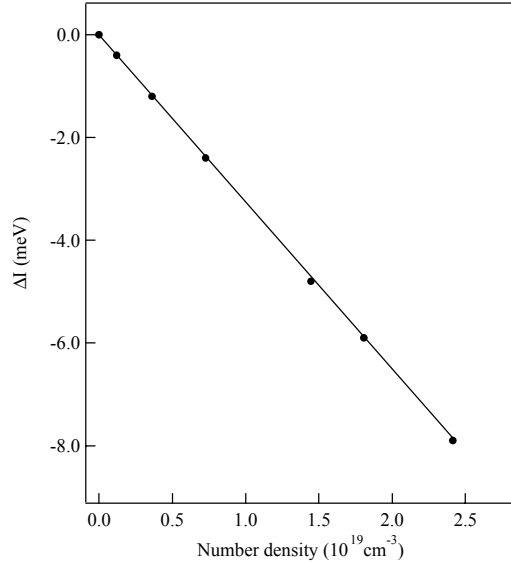


FIG 5. Shift of the second ionization energy of CH_3I , obtained from fitting the assigned spectra (e.g., Fig. 3) to the Rydberg equation, as a function of $c\text{-C}_4\text{F}_8$ number density. (The error in the energy for each point is ± 3 meV.)

following the same prescription as that described above for CF_4 gives a zero-kinetic-energy electron scattering length of $A = -0.618 \pm 0.012$ nm for $c\text{-C}_4\text{F}_8$. Therefore, the zero-kinetic-energy electron scattering cross-section for $c\text{-C}_4\text{F}_8$ is $\sigma = 4.8 \pm 0.2 \times 10^{-14} \text{ cm}^2$ from eq. (4). Recent attempts by Sanabia and co-workers [29] to measure the low energy electron scattering cross-section gave $\sigma = 4.8 \times 10^{-15} \text{ cm}^2$ for an electron energy of 1 eV. However, the sharp increase in the electron scattering cross-section of $c\text{-C}_4\text{F}_8$ below 1 eV made the extrapolation of the zero-kinetic-energy

Table 2. Selected second ionization energies (obtained from photoionization measurements) of CH_3I doped into various number densities ρ (10^{19} cm^{-3}) of $c\text{-C}_4\text{F}_8$.

ρ	I_2 (eV)
0.12	10.163
0.36	10.162
0.73	10.161
1.45	10.158
1.81	10.157
2.42	10.156

electron scattering cross-section from these low energy electron measurements unreliable [28].

In summary, we have presented photoionization and photoabsorption spectra of CH_3I and $\text{C}_2\text{H}_5\text{I}$ doped into CF_4 and *c*- C_4F_8 . From the perturber-induced density-dependent energy shifts of the ionization energies of the dopant molecules, we obtained the zero-kinetic-energy electron scattering lengths and electron scattering cross-sections for both CF_4 and *c*- C_4F_8 . We have also illustrated that the method of perturber-induced energy shifts of dopant high-*n* Rydberg states and ionization energies

continues to be an accurate means for determining the zero-kinetic-energy electron scattering lengths when other methods (e.g., the electron swarm method) fail.

Acknowledgements

This work was carried out at the University of Wisconsin Synchrotron Radiation Center (NSF DMR95-31009) and was supported by a grant from the Louisiana Board of Regents Support Fund (LEQSF (1997-00)-RD-A-14).

1. M. T. do N. Varella, A. P. P. Natalense, M. H. F. Bettega, and M. A. P. Lima, *Phys. Rev. A* **60**, 3684 (1999).
2. R. K. Jones, *J. Chem. Phys.* **84**, 813 (1986).
3. L. G. Christophorou, J. K. Olthoff and M. V. V. S. Rao, *J. Phys. Chem. Ref. Data* **25**, 1341 (1996).
4. A. A. Christodoulides, L. G. Christophorou, R. Y. Pai and C. M. Tung, *J. Chem. Phys.* **70**, 1156 (1979).
5. G. P. Karwasz, R. S. Brusa, A. Piazza and A. Zecca, *Phys. Rev. A* **59**, 1341 (1999).
6. Y. H. Jiang, J. F. Sun and L. Wan, *Phys. Rev. A* **52**, 398 (1995).
7. R. A. Morris, T. M. Miller, A. A. Viggiano, J. F. Paulson, S. Solomon and G. Reid, *J. Geophys. Res.* **100**, 1287 (1995).
8. D. M. Manos and D. L. Flamm, *Plasma Etching* (Academic Press, Boston, 1989).
9. L. E. Kline and M. J. Kushner, *Crit. Rev. Solid State Mater. Sci* **16**, 1 (1989).
10. J. W. Gallagher, E. C. Beaty, J. Dutton and L. C. Pitchford, *J. Phys. Chem. Ref. Data* **12**, 109 (1983).
11. A. V. Vasenkov, *J. Appl. Phys.* **85**, 1222 (1999).
12. J. A. Tossell and J. W. Davenport, *J. Chem. Phys.* **80**, 813 (1984); Erratum **83**, 4824 (1985).
13. A. M. Köhler, Ph.D. Dissertation, Hamburg University, Germany, 1987.
14. E. Fermi, *Nuovo Cimento* **11**, 157 (1934).
15. V. A. Alekseev and I. I. Sobel'man, *Sov. Phys. JETP* **22**, 882 (1966).
16. A. M. Köhler, R. Reininger, V. Saile and G. L. Findley, *Phys. Rev. A* **35**, 79 (1987).
17. C. M. Evans, R. Reininger and G. L. Findley, *Chem. Phys. Lett.* **297**, 127 (1998).
18. U. Asaf, I. T. Steinberger, J. Meyer and R. Reininger, *J. Chem. Phys.* **95**, 4070 (1991).
19. C. M. Evans, R. Reininger and G. L. Findley, *Chem. Phys.* **241**, 239 (1999).
20. A. K. Al-Omari, Ph. D. Dissertation, University of Wisconsin-Madison, Wisconsin, 1996.
21. A. K. Al-Omari and R. Reininger, *J. Chem. Phys.* **103**, 506 (1995).
22. C. M. Evans, Ph.D. Dissertation, Louisiana State University, Louisiana, 2001.
23. J. Meyer, R. Reininger, U. Asaf and I. T. Steinberger, *J. Chem. Phys.* **94**, 1820 (1991).
24. N. Knoblauch, A. Strobel, I. Fischer and V. E. Bondybey, *J. Chem. Phys.* **103**, 5417 (1995).
25. G. Herzberg, *Electronic Spectra and Electronic Structure of Polyatomic*

- Molecules* (Krieger, Malabar, FL, 1991).
26. T. K. Bose, J. S. Sochanski and R. H. Cole, *J. Chem. Phys.* **57**, 3592 (1972).
 27. J. W. Davenport, W. Ho and J. R. Schrieffer, *Phys. Rev. A* **21**, 85 (1980).
 28. L. Kevan and J. H. Futrell, *J. Chem. Soc. Faraday Trans. 2* **68**, 1742 (1972).
 29. J. E. Sanabia, G. D. Cooper, J. A. Tossell and J. H. Moore, *J. Chem. Phys.* **108**, 389 (1998).